

Enzymatic Extender Unit Generation for In Vitro Polyketide Synthase Reactions: Structural and Functional Showcasing of *Streptomyces coelicolor* MatB

Amanda J. Hughes¹ and Adrian Keatinge-Clay^{1,*}¹Department of Chemistry and Biochemistry, University of Texas at Austin, Austin, TX 78712, USA

*Correspondence: adriankc@mail.utexas.edu

DOI 10.1016/j.chembiol.2010.12.014

SUMMARY

In vitro experiments with modular polyketide synthases (PKSs) are often limited by the availability of polyketide extender units. To determine the polyketide extender units that can be biocatalytically accessed via promiscuous malonyl-CoA ligases, structural and functional studies were conducted on *Streptomyces coelicolor* MatB. We demonstrate that this adenylate-forming enzyme is capable of producing most CoA-linked polyketide extender units as well as pantetheine- and N-acetylcysteamine-linked analogs useful for in vitro PKS studies. Two ternary product complex structures, one containing malonyl-CoA and AMP and the other containing (2*R*)-methylmalonyl-CoA and AMP, were solved to 1.45 Å and 1.43 Å resolution, respectively. MatB crystallized in the thioester-forming conformation, making extensive interactions with the bound extender unit products. This first structural characterization of an adenylate-forming enzyme that activates diacids reveals the molecular details for how malonate and its derivatives are accepted. The orientation of the α -methyl group of bound (2*R*)-methylmalonyl-CoA, indicates that it is necessary to epimerize α -substituted extender units formed by MatB before they can be accepted by PKS acyltransferase domains. We demonstrate the in vitro incorporation of methylmalonyl groups ligated by MatB to CoA, pantetheine, or N-acetylcysteamine into a triketide pyrone by the terminal module of the 6-deoxyerythronolide B synthase. Additionally, a means for quantitatively monitoring certain in vitro PKS reactions using MatB is presented.

INTRODUCTION

Polyketides are secondary metabolites produced by diverse microbes that have been employed as antibiotics, antifungals, anticancer agents, and as many other types of therapeutics (Khosla et al., 2007; Walsh, 2004; Pfeifer and Khosla, 2001; Staunton and Wilkinson, 2001). Many of these metabolites are

produced by enzymatic assembly lines known as modular polyketide synthases (PKSs). Each PKS module is a collection of domains that catalyze the condensation and processing of small carbon building blocks, called extender units. Within a module, an acyltransferase (AT) selects an extender unit, a ketosynthase (KS) catalyzes the condensation reaction, and optional β -carbon processing enzymes, such as a ketoreductase (KR), a dehydratase (DH), and an enoylreductase (ER), set the functional groups and stereochemistries at the α - and β -carbons. The growing polyketide chain is shuttled through the PKS in a hand-over-hand fashion via an ~ 18 Å phosphopantetheinyl arm attached to the acyl carrier protein (ACP) of each module. The tremendous diversity of polyketide metabolites produced by modular PKSs largely results from extender unit selection (Figure 1A). Modular PKSs select two types of extender units: CoA-linked and ACP-linked (Chan et al., 2009). The most commonly selected extender units are CoA-linked, such as malonyl-CoA, (2*S*)-methylmalonyl-CoA, and (2*S*)-ethylmalonyl-CoA. The less common ACP-linked extender units, such as (2*R*)-methoxymalonyl-ACP, (2*R*)-hydroxymalonyl-ACP, and (2*S*)-aminomalonyl-ACP, are synthesized on the phosphopantetheinyl arm of an ACP separate from the PKS assembly line (Chan and Thomas, 2010).

To study the activities of PKS modules in vitro, a supply of polyketide extender units is necessary; however, the cost and availability of these molecules is prohibitive. If the extender units are obtained from a commercial source, experiments designed to produce over a milligram of polyketide product in vitro become impractical. An alternative is to use N-acetylcysteamine (SNAC)-linked extender units, which have been employed in feeding studies and in vitro reactions (Carroll et al., 2002; Pohl et al., 1998). Pohl et al. (1998) showed that on incubation of synthetic (2*RS*)-methylmalonyl-SNAC with DEBS3, the third protein of the 6-deoxyerythronolide B synthase, in the presence of (2*S*, 3*R*)-3-hydroxy-2-methylpentanoate-SNAC and NADPH, the anticipated triketide lactone was generated; this result indicates that the terminal DEBS3 AT accepts methylmalonyl units from (2*S*)-methylmalonyl-SNAC. To access CoA-linked extender units enzymatically, Pohl and coworkers utilized the malonyl-CoA synthetase MatB from *Rhizobium trifolii*, which has a broad substrate tolerance, and demonstrated that it can produce malonyl-CoA, methylmalonyl-CoA, ethylmalonyl-CoA, as well as unnatural extender units such as cyclopropylmalonyl-CoA, cyclobutylmalonyl-CoA, benzylmalonyl-CoA, and cyclopropylmethylenemalonyl-CoA (Pohl et al., 2001). We have employed the previously uncharacterized *Streptomyces*

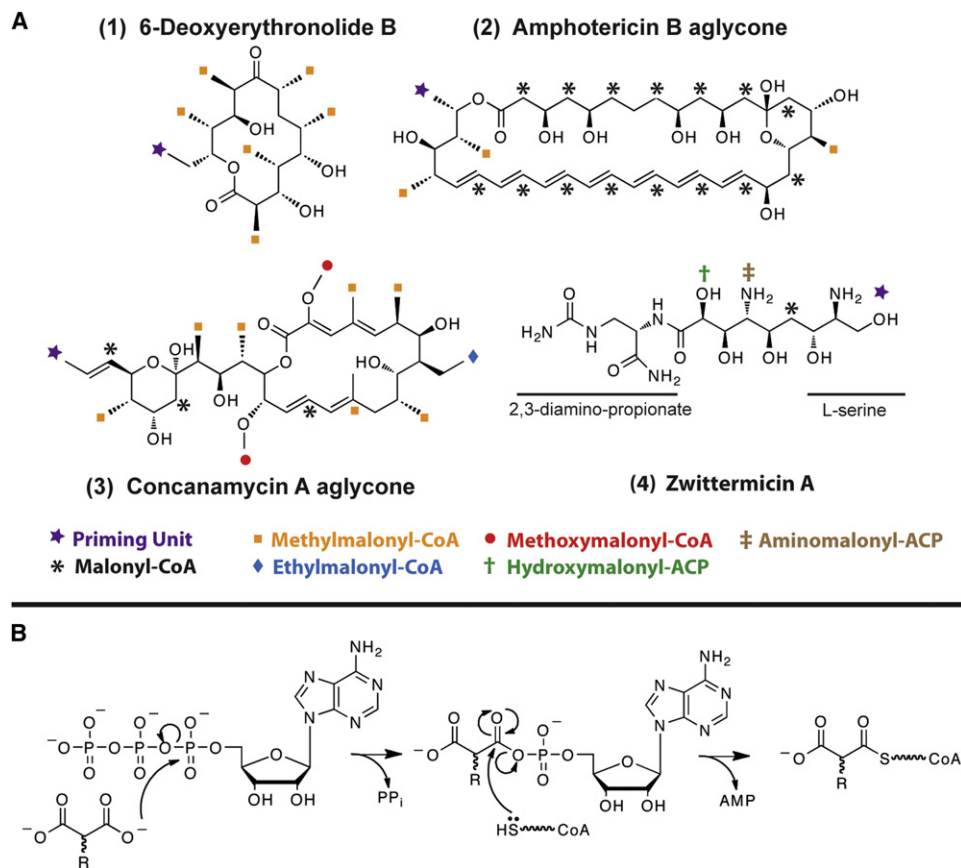


Figure 1. Polyketide Extender Unit Incorporation and MatB Reaction

(A) The most common CoA-linked polyketide extender units are mCoA, (2S)-mmCoA, and (2S)-emCoA; the most common ACP-linked polyketide extender units are (2R)-oxACP, (2R)-hmACP, and (2S)-amACP. These extender units are incorporated into polyketides 1–3 and a polyketide-nonribosomal peptide hybrid, 4. ★, Priming unit; *, mCoA; ■, mmCoA; ◆, emCoA; ●, oxACP; ‡, amACP; †, hmACP.

(B) Two-step reaction mechanism of *Streptomyces coelicolor*. MatB: In the adenylation-forming reaction, the ATP α -phosphate is attacked by a malonate derivative carboxylate to form the adenylation intermediate and pyrophosphate. In the thioester-forming reaction, CoA displaces AMP to produce the extender unit and AMP.

coelicolor MatB to synthesize CoA-linked extender units and derivatives thereof (Figure 1B).

The *S. coelicolor* malonyl-CoA synthetase MatB is an adenylation-forming enzyme that is best classified with acyl-CoA synthetases. MatB is anticipated to be enzymatically and structurally homologous to such enzymes as acyl-CoA synthetases (Protein Data Bank [PDB] codes: 3EQ6, 1V26, 1PG3, 1RY2)(Kochan et al., 2009; Hisanaga et al., 2004; Gulick et al., 2003; Jogl and Tong, 2004), 4-chlorobenzoyl-CoA ligase (PDB code: 1T5D)(Gulick et al., 2004), the adenylation domains (A-domains) of nonribosomal peptide synthetases (NRPSs; PDB codes: 3ITE, 3E7W, 1AMU)(Lee et al., 2010; Yonus et al., 2008; Conti et al., 1997; Strieker et al., 2010; Mootz et al., 2002; Marahiel, 2009), and firefly luciferase (PDB code: 2D1R)(Nakatsu et al., 2006). A structure of a diacid-activating adenylation-forming enzyme has not yet been reported. Reactions catalyzed by adenylation-forming enzymes can be represented by a medium-chain acyl-CoA synthetase: in the adenylation-forming conformation a medium-sized fatty acid is selected to attack the α -phosphoryl moiety of adenosine triphosphate (ATP) via its carboxylate to yield an

acyl-adenylate and pyrophosphate; in the thioester-forming conformation the thiol acceptor CoA is selected to perform the second half-reaction, generating acyl-CoA and AMP (Kochan et al., 2009).

Here, we demonstrate the *S. coelicolor* MatB-catalyzed synthesis of polyketide extender units malonyl-CoA (mCoA), methylmalonyl-CoA (mmCoA), ethylmalonyl-CoA (emCoA), methoxymalonyl-CoA (oxCoA), and hydroxymalonyl-CoA (hmCoA), marking the first enzymatic syntheses of oxCoA and hmCoA. Equivalent pantetheine- (PANT-) and SNAC-linked extender units were also generated, demonstrating that MatB is not only promiscuous toward malonyl derivatives, but also thiol acceptors. Crystal structures of two MatB ternary product complexes were obtained with malonyl-CoA and AMP (1.45 Å resolution) and with (2R)-methylmalonyl-CoA and AMP (1.43 Å resolution). These are the first structures of a diacid-activating adenylation-forming enzyme. The strong electron density surrounding the protein, thioester product, and AMP provides some of the most complete snapshots of product formation in the enzyme superfamily. The orientation of the (2R)-methylmalonyl-CoA

α -methyl group reveals the stereoselectivity of MatB toward α -substituted malonate derivatives and also reveals the pocket that enables MatB to be promiscuous toward α -substituents. In vitro reactions in which the methylmalonyl groups of MatB-synthesized extender units mmCoA, mmPANT, and mmSNAC are incorporated into a triketide pyrone by the final module of the 6-deoxyerythronolide B synthase exemplify the use of MatB. A protocol for monitoring such reactions through a coupled reaction, also catalyzed by MatB, is described.

RESULTS

MatB Synthesizes Diverse CoA-, PANT-, and SNAC-Linked Extender Units

Products from incubations of CoA and a diacid (malonic acid, methylmalonic acid, ethylmalonic acid, methoxymalonic acid, and tartronic acid) with MatB were collected during high-performance liquid chromatography (HPLC) runs and analyzed by mass spectrometry. The observed masses (calculated masses) from the hmCoA, oxCoA, mCoA, mmCoA, and emCoA reactions were 867.8(868.1), 881.9(882.1), 851.7(852.1), 865.9(866.1), and 879.9(880.1), respectively, indicating the production of each of the five CoA-linked extender units (Figure 2A). Aminomalonyl-CoA could not be produced. MatB was also found capable of synthesizing PANT- and SNAC-linked extender units; employing identical HPLC methanol gradients, the retention times of the PANT-linked extender units were increased relative to the CoA-linked extender units, whereas the retention times of the SNAC-linked extender units were decreased (Figures 2B and 2C). Two product peaks were observed in each of the hmCoA, hmPANT, and hmSNAC reactions. Both peaks from the hmSNAC reaction were collected and subjected to LC/MS analysis. The observed masses (calculated masses) of 222.2 (222.0) and 206.2(206.1), correspond to hmSNAC and mSNAC, respectively. The mSNAC peak may have resulted from a malonic acid impurity in the tartronic acid stock. With the addition of sufficient ATP, thiol, and diacid, MatB reactions can be scaled up to yield multimilligram quantities that can be readily analyzed by nuclear magnetic resonance (NMR). In summary, *S. coelicolor* MatB produces each of the CoA-, PANT-, and SNAC-linked extender units mCoA, mmCoA, emCoA, oxCoA, hmCoA, mPANT, mmPANT, emPANT, oxPANT, hmPANT, mSNAC, mmSNAC, emSNAC, oxSNAC, and hmSNAC.

Incorporation of MatB-synthesized mmCoA, mmPANT, and mmSNAC into a Triketide Pyrone

The final module and thioesterase from the 6-deoxyerythronolide B synthase (Mod6TE) has been used in previous experiments to produce triketide lactones (Pohl et al., 1998; Gokhale et al., 1999; Menzella et al., 2005). We were able to incorporate methylmalonate from MatB-synthesized mmCoA, mmPANT, and mmSNAC into a triketide pyrone by (1) incubating MatB ligation reactions overnight at 22°C; (2) adding Mod6TE, *S. coelicolor* methylmalonyl-CoA epimerase (Dayem et al., 2002), and (2*S*, 3*R*)-2-methyl-3-oxopentanoate-SNAC (Keatinge-Clay, 2007); and (3) incubating at least 1 day at 22°C and analyzing for polyketide production via HPLC (Figures 2D–2F). To confirm the identity of the triketide pyrone, the fraction corresponding to the largest peak (at 290 nm) was collected and subjected to LC/MS; the

observed mass (calculated mass) of the triketide pyrone was 169.2(169.1). In all reactions, mmSNAC is formed as a byproduct generated by MatB using methylmalonate and SNAC liberated from (2*S*, 3*R*)-2-methyl-3-oxopentanoate-SNAC, although thioesterase-catalyzed hydrolysis of (2*S*, 3*R*)-2-methyl-3-oxopentanoate-SNAC may also contribute to mmSNAC formation (Figure 2E) (Wang et al., 2009). Monitoring mmSNAC production represents a powerful, new method of following in vitro PKS reactions, especially those producing polyketides lacking chromophores.

Overall MatB Structure

The conditions that yielded protein crystals contained all of the substrates required for the synthesis of mCoA or mmCoA as described in the Experimental Procedures. Briefly, purified protein was incubated with the substrates of the MatB reaction: ATP, magnesium, CoA, and malonate or methylmalonate. Clusters of elongated, orthorhombic crystals, often hollowed along their long axes, grew overnight. Diffraction data was collected using crystals flash-frozen in their mother liquor. Molecular replacement proved unsuccessful, as is often the case with adenylate-forming enzymes (Shah et al., 2009). The mCoA/AMP-bound MatB structure was solved via single-wavelength anomalous dispersion using selenomethionine-labeled protein. The native malonyl-CoA/AMP-bound and methylmalonyl-CoA/AMP-bound complexes were then refined at resolutions of 1.45 Å and 1.43 Å, respectively (Table 1). A comparison of the ternary complexes yields root-mean-square deviation of 0.06 Å.

MatB is comprised of 485 residues, possesses a molecular weight of 50.6 kDa, and is monomeric as determined through gel filtration chromatography and through an analysis of the packing within the crystals. Like other adenylate-forming enzymes, MatB has a large N-terminal body (residues 1–387) and a small C-terminal lid (residues 388–485), yet is the smallest of the adenylate-forming enzymes solved to date (Figure 3A). No density was observed for the N-terminal histidine tag, residues 1–3, or residues 472–485 of the C-terminal lid. No density for the 3',5'-diphosphoadenosine of CoA was observed either, permitting only the phosphopantetheine moiety of CoA to be modeled. The overall structure for mCoA/AMP-bound MatB contains 467 residues, 348 waters, 1 mCoA, 1 AMP molecule, and 1 solvated Mg²⁺ in the asymmetric unit. The overall structure of mmCoA/AMP-bound MatB contains 467 residues, 407 water molecules, 1 mmCoA, 1 AMP molecule, and 1 solvated Mg²⁺ in the asymmetric unit. The electron density clearly reveals an *R* stereochemistry at the α -carbon indicating that (2*R*)-mmCoA is bound. Other than the α -methyl group, the positions of the bound mCoA and (2*R*)-mmCoA extender units are superimposable between the two structures.

MatB Observed in the Thioester-Forming Conformation

Adenylate-forming enzymes can adopt at least two catalytically distinct conformations (Reger et al., 2008; Kochan et al., 2009; Lee et al., 2010). The C-terminal lid pivots 140° between the two catalytically-active conformations (the adenylate-forming conformation and the thioester-forming conformation) in a process termed “domain alternation” (Reger et al., 2008; Shah et al., 2009) (Figure 3A). An aspartate located in a linker between the N-terminal body and the C-terminal lid of

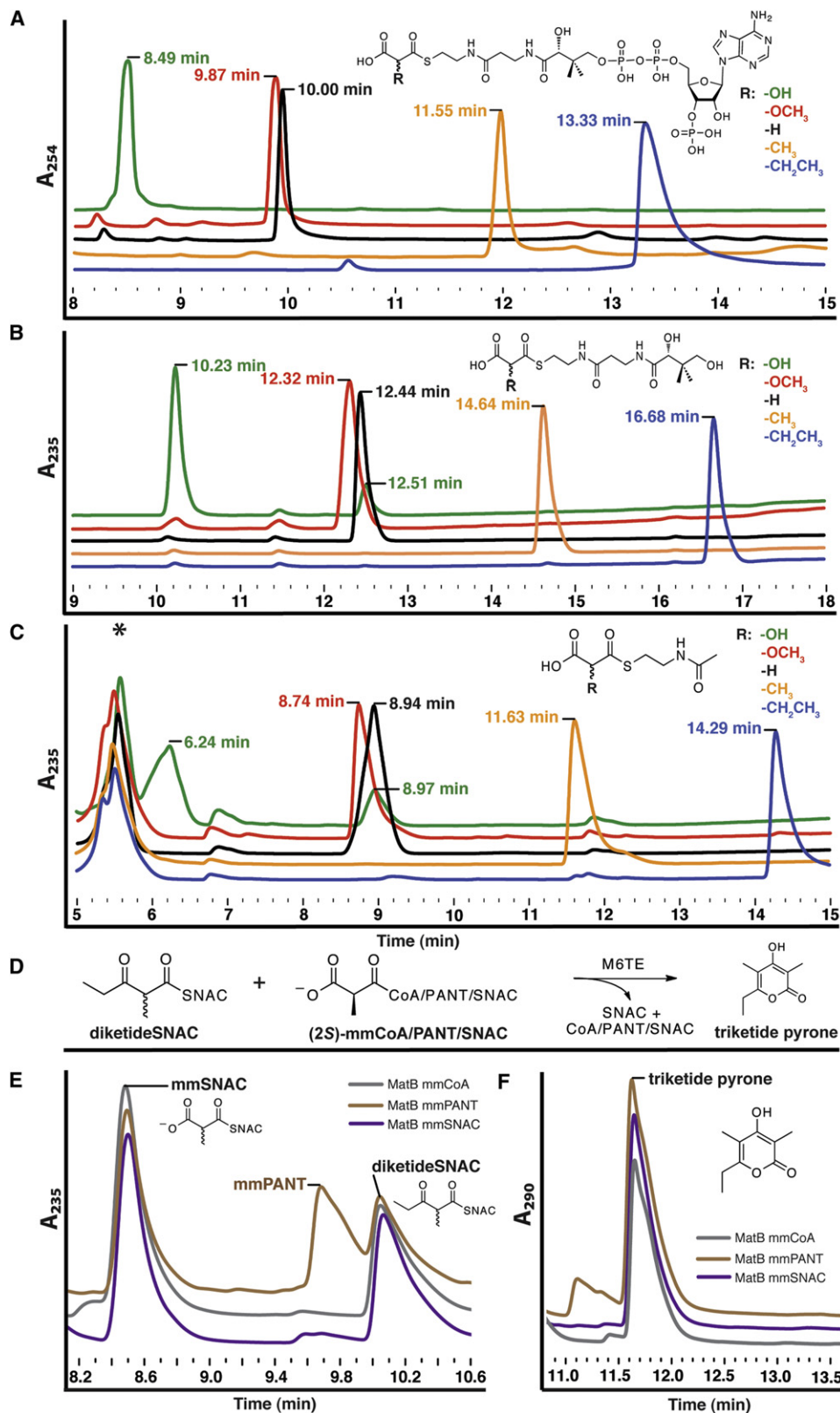


Figure 2. HPLC Analysis of MatB and Mod6TE Reactions

(A–C) MatB synthesized 15 polyketide extender units valuable for in vitro PKS reactions. Retention times (min) of extender units formed using CoA, PANT, and SNAC as the thiol acceptor are indicated. The observed masses (calculated masses) from the hmCoA, oxCoA, mCoA, mmCoA, and emCoA reactions were

adenylate-forming enzymes, is usually considered to be the principle pivot point about which the C-terminal lid rotates during domain alternation and is hypothesized to interact with the arginine that is the final residue of the N-terminal body in the thiolation conformation (Wu et al., 2008). The thioester-forming conformation of 4-chlorobenzoate CoA ligase shows an ionic interaction between hinge residue D402 and the final residue of the N-terminal body (R400); the D402P and D402A mutants showed decreased catalytic activity (Reger et al., 2008; Wu et al., 2008). The putative hinge residue in MatB is D387, which is four residues after the final residue of the N-terminal body (R383) and highly conserved among malonyl-CoA synthetases. The side-chain electron density for the MatB linker (residues 384–388, KATDL) is too weak to observe interactions with R383.

Comparison to Adenylate-Forming Enzyme Core Motifs

Highly conserved regions of adenylate-forming enzymes have been categorized into ten major core motifs (A1–A10, Table 2) (Marahiel et al., 1997). Motif A3 contains a serine/threonine-rich region hypothesized to interact with the β - and γ -phosphates of ATP during the adenylation reaction, stabilizing the release of pyrophosphate; *S. coelicolor* MatB contains an equivalent region (Marahiel et al., 1997). The role of motifs A4 and A5 are to bind the carboxylate substrate and stabilize the formation of the adenylate intermediate; ten residues, mostly located between these motifs, have been identified as “specificity-conferring residues” that form the binding site for a carboxylate substrate (Stachelhaus et al., 1999). A conserved aspartate in motif A4 of A-domains (FDXS) ionically interacts with the α -amino group of bound amino acids; in *S. coelicolor* MatB, the corresponding residue is V188 (HVHG) (PDB codes: 1AMU and 3E7W) (Conti et al., 1997; Yonus et al., 2008). H189, also within *S. coelicolor* MatB motif A4, coordinates with the specificity-conferring residues S261 and R238 to help form the malonate binding pocket. Within the *S. coelicolor* MatB motif A5 (ERYGMTE), R238 forms a salt bridge with the extender unit carboxylate in each of the ternary product complex structures; the corresponding residue in the phenylalanine-selective A-domain of the gramicidin synthetase is A322 (NAYGPTE), which helps create a large hydrophobic pocket for the phenylalanine side chain (PDB code: 1AMU) (Conti et al., 1997). Interestingly, the loop immediately following motif A5, which contains two specificity-conferring residues, is one residue shorter in *S. coelicolor* MatB than in most adenylate-forming enzymes. Thus, the position of the specificity-determining residue M291 in *S. coelicolor* MatB is slightly different than the most equivalent residue, C331, in the phenylalanine-activating A-domain of the gramicidin synthetase. In terms of length and orientation, the loop following motif A5 that is most

similar to that of *S. coelicolor* MatB is from a medium-chain adenylate-forming enzyme (PDB code: 3EQ6) (Kochan et al., 2009).

Bound Malonyl-CoA and Methylmalonyl-CoA

Both mCoA and (2*R*)-mmCoA products are bound between the N-terminal body and C-terminal lid of MatB (Figure 3D). Although a few adenylate-forming enzymes have been solved with CoA or thioester products bound (PDB codes: 2P2F, 1PG4, 3EQ6) (Reger et al., 2007; Gulick et al., 2003; Kochan et al., 2009), the MatB complex structures presented here provide the strongest density for a phosphopantetheinyl arm to date. In both structures, the bound extender unit displays electron density that continues past the CoA β -phosphoryl moiety and possesses an average B-factor lower than the average B-factor of MatB. The interactions with the extender unit products can be divided into three categories:

1. Malonyl groups are bound primarily by residues S261 and R283 (Figure 3E). The presence of the arginine in core motif A5 is a hallmark of malonyl-CoA synthetases. Indeed, R283 serves an important functional role: the ternary complexes reveal that it forms strong ionic interactions with the carboxylates of both mCoA and mmCoA (another active site arginine forms strong ionic interactions with this carboxylate in ATs when the extender unit is selected for transfer to an ACP [Tang et al., 2006]). The observed ψ and ϕ angles for S261 are -17.9° and 88.5° , respectively; that these values are outside of the expected Ramachandran regions suggests the importance of S261 in the MatB reaction (Herzberg and Moulton, 1991). In the ternary complexes presented in this work, S261 participates in a hydrogen-bonding network that includes R283 and the extender unit carboxylate (Figure 3E).
2. The pantetheine arm is contacted by hydrogen bonds from the backbone carbonyls of residues G392 and G393 as well as hydrophobic interactions principally mediated by Y384 (as observed in a medium-chain acyl-CoA synthetase ternary complex, PDB code: 3EQ6) (Figure 3F) (Kochan et al., 2009). The A8 core motif, which contains these residues, is hypothesized to possess multiple functions: in the adenylate-forming conformation, the first arginine may help stabilize the pyrophosphate leaving group; in the thioester-forming conformation, it may interact with the pantetheinyl arm, as observed in the MatB structure.
3. The CoA β -phosphate is ionically bound by R236 and R461 (Figure 3G). A third arginine, R459, may form ionically interact with the CoA α -phosphate as it is within 6 Å.

867.8(868.1), 881.9(882.1), 851.7(852.1), 865.9(866.1), and 879.9(880.1), respectively. The two peaks observed for hmSNAC at 6.24 and 8.97 min were analyzed by positive-ESI LC/MS and correspond to hmSNAC (222.2(222.0)) and mSNAC (206.2(206.1)); the presence of mSNAC is may be from a malonate impurity in the tartronic acid stock. *AMP.

(D) Mod6TE reaction. The selection of (2*S*)-mmCoA/PANT/SNAC extender unit and transthioesterification of (2*S*, 3*R*)-2-methyl-3-oxopentanoate-SNAC (diketideSNAC) releases CoA/PANT/SNAC and SNAC, respectively. The condensation reaction results in the formation of a triketide, which cyclizes to generate a triketide pyrone.

(E) HPLC analysis of Mod6TE reactions at 235 nm. The formation of mmSNAC (from the transthioesterification of diketide-SNAC) may be used as a diagnostic tool to follow an in vitro PKS reaction.

(F) HPLC analysis of Mod6TE reactions at 290 nm. Triketide pyrone was synthesized from all three different extender units, (2*S*)-mmCoA/PANT/SNAC. The identity of triketide pyrone was confirmed by positive-ESI LC/MS with an observed mass (calculated mass) of 169.2(169.1).

Table 1. Data Collection and Refinement of *S. coelicolor* MatB Structures

	MatB (Malonyl-CoA) 3NYR	MatB (2 <i>R</i> -Methylmalonyl-CoA) 3NYQ	SeMatB (2 <i>R</i> -Methylmalonyl-CoA)
Space group	C222(1)	C222(1)	C222(1)
Cell dimensions			
<i>a</i> , <i>b</i> , <i>c</i> (Å)	73.2, 86.6, 153.1	73.4, 86.8, 153.4	73.9, 87.4, 154.4
$\alpha = \beta = \gamma$ (°)	90	90	90
Resolution (Å)	50–1.45	50–1.43	50–1.75
R _{merge}	0.051 (0.439)	0.062 (0.292)	0.080 (0.202)
I/σ(I)	23.1 (2.6)	15.5 (3.9)	30.8 (7.1)
Completeness (%)	99.8 (99.4)	98.5 (82.4)	97.8 (94.7)
Redundancy	7.1 (4.5)	6.8 (3.8)	3.9 (4.0)
Refinement			
Resolution (Å)	50–1.45	50–1.43	50–1.75
Unique reflections	621,987	671,166	537,849
R _{work} /R _{free}	0.1997/0.2247	0.1951/0.2161	0.2026/0.2353
Ramachandran allowed, outlier (%)	99.34, 0.66	99.34, 0.66	99.55, 0.45
Number of atoms			
Protein	3378	3378	3320
Extender unit	28	29	29
AMP	23	23	N/A
Water	347	404	338
B factors (Å ²)			
Protein	16.72	17.40	19.66
Extender unit	14.60	14.29	21.06
AMP	21.94	23.79	N/A
Water	26.50	27.64	27.75
Rmsd			
Bond lengths (Å)	0.010	0.013	0.011
Bond angles (°)	1.80	1.77	1.45
Highest Res. Bin (Å)	1.49–1.45	1.47–1.43	1.78–1.75

AMP: adenosine monophosphate; rmsd: root-mean-square deviation.

Bound Adenosine Monophosphate

AMP is bound in the MatB ternary complex structures at a site equivalent to that observed in other adenylate-forming enzymes (e.g., PDB codes: 3EQ6, 1MD9, 3E7W, 1AMU, 2P2F, 3FCC). The 2F_o-F_c electron density maps (contoured at $\sigma = 1.6$) do not completely surround AMP; however, the overall B-factors for AMP in the mCoA- and mmCoA-bound MatB structures are 22 Å² and 23 Å², respectively, which is only slightly higher than the average B-factors for the MatB residues (16.6 Å² and 17.3 Å², respectively) (Figure 4B). The distance from the thioester carbon to the nearest oxygen atom of the AMP phosphate, which had been covalently bonded to one another in the adenylate intermediate, is ~3.6 Å. Positively-charged K390 and K395 form ionic interactions with the AMP α -phosphate, whereas T287 also forms a hydrogen bond with it (Figure 4E). The backbone carbonyl of R283 forms a hydrogen bond to the N7-amine of adenine, while a conserved aspartic acid, D368, interacts with both AMP hydroxyl groups (Figure 4C).

DISCUSSION

Malonyl-CoA synthetases are capable of generating many extender units for in vitro PKS reactions. *R. trifolii* MatB is

frequently used to generate malonyl-CoA for PKSs that utilize α -unsubstituted extender units (Gao et al., 2010). Here, we have demonstrated that *S. coelicolor* MatB, like *R. trifolii* MatB, ligates diverse malonate derivatives to CoA to generate a diversity of α -substituted polyketide extender units that are utilized by modular PKSs. We have shown that *S. coelicolor* MatB is also promiscuous toward thiol acceptors, as established by the synthesis of PANT- and SNAC-linked extender units. These extender units are nearly as efficient as CoA-linked extender units at transferring malonate derivatives to PKS modules, as demonstrated by our experiments using Mod6TE in the production of a triketide pyrone (Figure 2F).

In an effort to understand the nature of the promiscuity of MatB toward malonate derivatives and thiol acceptors, as well as the stereoselectivity imposed by MatB toward α -substituted malonate derivatives, the structures of two MatB ternary product complexes were obtained. These structures, combined with information from analyses of more thoroughly studied adenylate-forming enzymes, allow the following catalytic cycle to be proposed for MatB-catalyzed synthesis of malonyl-CoA: malonate and ATP bind to MatB, with the binding of ATP potentially causing the C-terminal lid to dock to the N-terminal body in

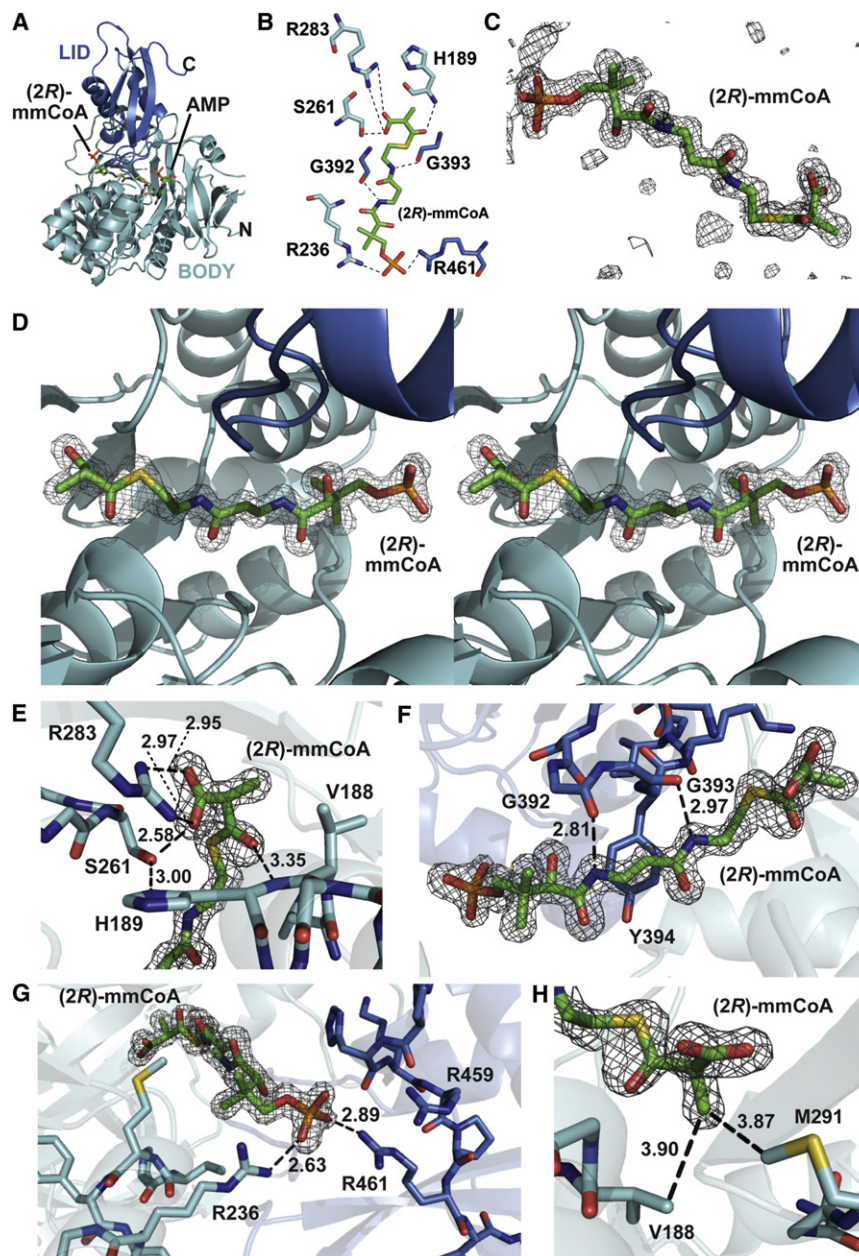


Figure 3. MatB Structure and Active Site Architecture

(A) Overall structure of the mmCoA/AMP/MatB ternary complex. The N-terminal body is colored light blue, the C-terminal lid is colored dark blue, and the N and C termini are indicated. (2R)-mmCoA and AMP are colored green.

(B) LIGPLOT representation of interactions observed between (2R)-mmCoA and surrounding MatB residues.

(C) Simulated-annealing omit map of (2R)-mmCoA (contoured at $\sigma = 3.0$).

(D) Stereodiagram of (2R)-mmCoA in the pantetheine tunnel with surrounding $2F_o - F_c$ electron density map ($2F_o - F_c$ map contoured at $\sigma = 1.6$).

(E) H189, S261, and R283, in the N-terminal body, interact with methylmalonyl moiety of (2R)-mmCoA. A hydrogen-bonding network is formed between S261, R283, and the (2R)-mmCoA carboxylate (distances in Å, $2F_o - F_c$ map contoured at $\sigma = 1.6$).

(F) Carbonyls from G392 and G393 hydrogen bond with the pantetheine amide groups. Hydrophobic interactions are also formed between Y394 and the pantetheine (distances in Å, $2F_o - F_c$ map contoured at $\sigma = 1.6$).

(G) R236 and R461 form salt-bridges with the (2R)-mmCoA β -phosphate. No density was observed for the 3',5'-diphosphoadenosine; however, the positively charged pantetheine tunnel entrance likely interacts with both α - and β -phosphate groups (distances in Å, $2F_o - F_c$ map contoured at $\sigma = 1.6$).

(H) V188 and M291 form a hydrophobic pocket near the α -methyl substituent of (2R)-mmCoA (distances in Å, $2F_o - F_c$ map contoured at $\sigma = 1.6$).

the adenylate-forming conformation (Kochan et al., 2009). Malonate binds largely via a salt-bridge between one of its carboxylates and R283 and S261 (Figure 3E). By analogy with other adenylate-forming enzymes, MatB interacts with ATP by bonding to its phosphates with the serine/threonine-rich A3 core motif, its ribose with the conserved aspartate D368, and its adenine through van der Waals interactions with loop residues S261–A263 (Figures 4C and 4E). The free carboxylate of the malonate is positioned to attack the ATP α -phosphate, releasing pyrophosphate, which may be stabilized as a leaving group by K476 (Kochan et al., 2009). After pyrophosphate diffuses from the active site, the C-terminal lid pivots about D387 to adopt the thioester-forming conformation in which the “pantetheine

tunnel” is created. The malonyl-adenylate remains bound during this domain alternation process. CoA then binds through hydrogen bonds with the G392 and G393 carbonyls, hydrophobic interactions with Y394, and ionic interactions with R236 and R461 (Figures 3F and 3G). Inspection of the MatB structures does not reveal a site that recognizes the 3',5'-diphosphoadenosine of CoA as is observed other adenylate-forming enzymes (e.g., PDB codes: 1PG3 and 2P2F). The entry of CoA into the MatB active site is halted when the diphosphate moiety forms salt-bridges with positively charged residues at the tunnel opening (Figure 3G), although these ionic interactions are not required for catalysis because PANT and SNAC can serve as thiol acceptors. Because the pantetheinyl arm makes as many contacts to the C-terminal lid as it does with the N-terminal body, CoA likely enters the pantetheine tunnel after tunnel formation. After an attack of the CoA thiolate on the malonyl-adenylate carbonyl, the leaving group AMP, stabilized by K395, is generated. Finally, AMP and the malonyl-CoA extender unit diffuse out of the active site, aided by the pivoting motion of the C-terminal lid during domain alternation.

Table 2. Core Motifs Conserved in Adenylate-Forming Enzymes

Core	Function	Adenylate-Forming Enzyme Consensus Sequence	Corresponding MatB Sequence
A1	Structural	L(TS)YxEL	(29)LTYAEL(34)
A2	Structural	LKAGxAYL(VL)P(LI)D	(69)LLAGVAAVPLN(79)
A3	Stabilize pyrophosphate leaving group	LAYxxYTSG(ST)TGxPKG	(137)PALVVYTSGETTGPPKG(152)
A4	Asp interacts with α -amino groups of peptides	FDxS	(187)HVHG(190)
A5	Stabilize product	NxYGPTE	(282)ERYGMTE(288)
A6	Unknown	GELIxGxG(VL)ARGYL	(334)GEIQVRGPNLFTEYL(348)
A7	Stabilize ATP/AMP ribose	Y(RK)TGDL	(364)FRTGDM(369)
A8	Essential for adenylation	GRxDxQVKIRGxRIELGEIE	(382)GRKATDLIKSGGYKIGAGEIE(402)
A9	Unknown	LPxYM(I)V)P	(454)LAPHKRP(460)
A10	Stabilize ATP/AMP ribose	NGK(VL)DR	(474)MGKIMK(479)

AMP: adenosine monophosphate; ATP: adenosine triphosphate. Ten major conserved core motifs have been identified for the adenylate-forming enzymes (A1–A10) (Marahiel et al., 1997). Corresponding MatB sequences are listed for comparison.

The $2F_o - F_c$ electron density maps from the mmCoA/AMP-bound MatB ternary complex suggest that MatB forms (2*R*)-mmCoA and not (2*S*)-mmCoA. In related structures, the position of a bound AMP is similar to its position within the adenylate intermediate, thus this intermediate can be approximately reconstructed from the positions of the malonyl group and AMP (Reger

et al., 2007, 2008; Conti et al., 1997; Yonus et al., 2008; Hisanaga et al., 2004; Kochan et al., 2009). Due to the proximity of the α -substituent and the AMP phosphoryl moiety (~ 4 Å in the ternary product complex and likely closer within the adenylate intermediate), the stereochemistry of the α -carbon is limited to the *R*-configuration (Figure 5C). The formation of (2*R*)-mmCoA

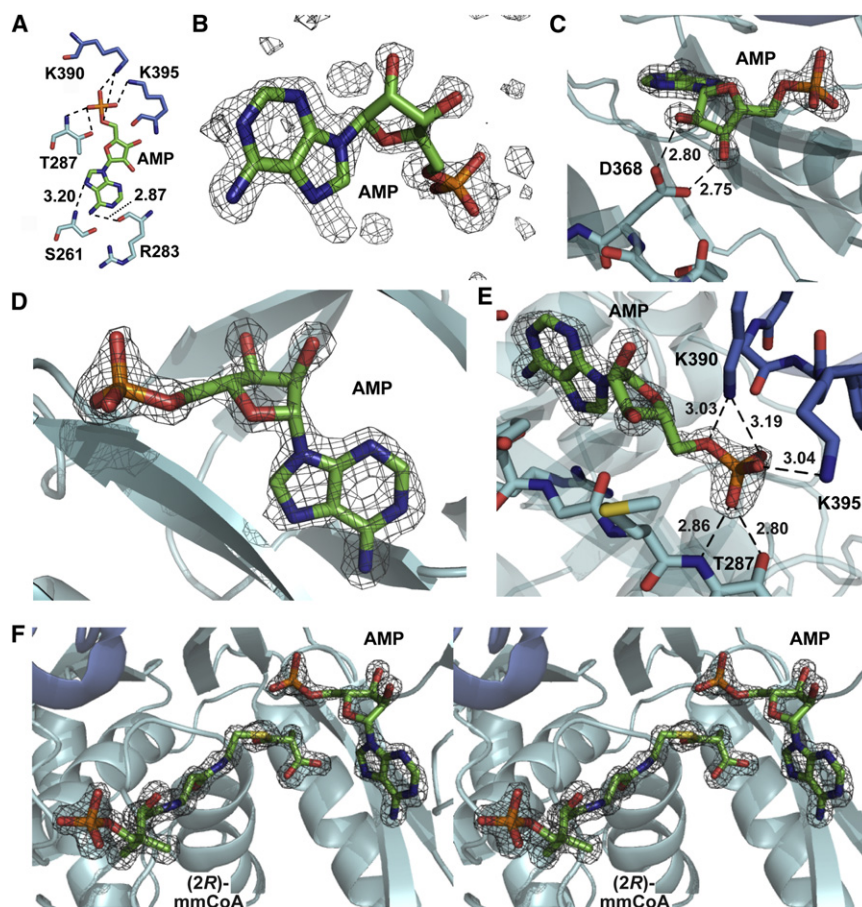


Figure 4. Adenosine Monophosphate Bound in the Ternary Complex

(A) LIGPLOT diagram of AMP and MatB interactions (distances in Å).

(B) Simulated-annealing omit map of AMP (contoured at $\sigma = 3.0$).

(C) Interaction between conserved D368 and hydroxyl groups of AMP ($2F_o - F_c$ map contoured at $\sigma = 1.6$).

(D) $2F_o - F_c$ electron density map surrounding AMP (contoured at $\sigma = 1.6$).

(E) Ionic interactions between the AMP α -phosphate and both K390 and K395. The backbone amide and hydroxyl group of T287 form hydrogen bonds with the AMP α -phosphate (distances in Å, $2F_o - F_c$ map contoured at $\sigma = 1.6$).

(F) Stereodiagram of (2*R*)-mmCoA and AMP within the active site (distances in Å, $2F_o - F_c$ map contoured at $\sigma = 1.6$).

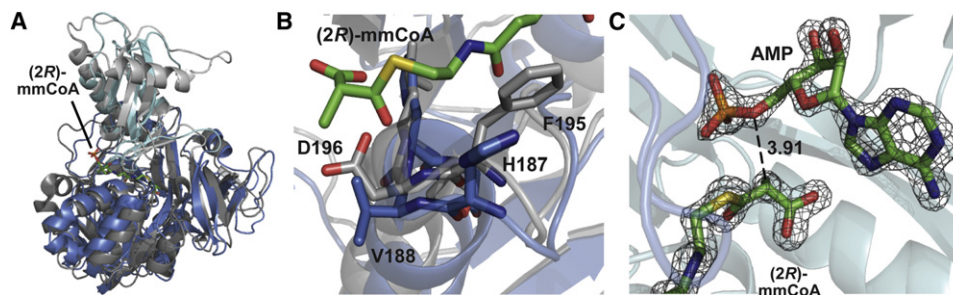


Figure 5. Engineering Substrate Specificity and Product Stereochemistry

(A) Structural alignment of MatB (blues) and DltA (greys, PDB code: 3E7W). DltA is an A-domain that ligates D-alanine onto the phosphopantetheinyl arm of a peptidyl carrier protein.

(B) D196 (gray) of the FDxS motif in DltA ionically interacts with the of D-alanine amino group. The MatB mutant V188D could catalyze the formation of aminomalonyl-CoA.

(C) The distance between the AMP leaving group and the α -carbon is 3.91 Å. Re-engineering MatB to form (2S)- α -substituted extender units may not be possible because the α -substituent of a (2S)- α -substituted-malonyl adenylate intermediate would clash with the AMP phosphoryl moiety. MatB is hypothesized to synthesize (2R)-mmCoA, (2R)-emCoA, (2R)-hmCoA, and (2R)-oxCoA (2F_o-F_c map contoured at $\sigma = 1.6$).

is consistent with observations from previous experiments that failed to synthesize polyketides from mmCoA produced by MatB in the absence of an epimerase (Murli et al., 2003). Thus, we hypothesize that MatB also synthesizes (2R)-emCoA, (2R)-hmCoA, and (2R)-oxCoA in a stereocontrolled manner. As the AT domains of PKSs are very stereoselective, only accepting (2S)-mmCoA and (2S)-emCoA, epimerization of mmCoA and emCoA is necessary for the incorporation of these MatB-synthesized extender units into PKSs and can be accomplished via spontaneous epimerization under acidic conditions or enzymatically-catalyzed epimerization through the addition of an epimerase (e.g., mmCoA epimerase) (Murli et al., 2003).

Organic syntheses of mSNAC, mmSNAC, oxSNAC, and hmSNAC have been reported (Pohl et al., 1998; Carroll et al., 2002); however, the syntheses of hmSNAC and oxSNAC involve multistep syntheses with 13% and 29% yields, respectively (Carroll et al., 2002). Using MatB, super-stoichiometric quantities of extender units can be enzymatically produced in situ to drive the synthesis of milligram quantities of polyketides from in vitro reactions. MatB also serves as an extender unit regeneration system, as supported by the formation of mmSNAC in the Mod6TE reactions. With the addition of excess diacid and ATP, MatB will continually regenerate product by recycling the appropriate thiol acceptor (e.g., CoA, PANT, or SNAC). The MatB-catalyzed formation of α -substituted extender units enables the generation of otherwise unavailable isotopically- or radioactively-labeled extender units for more detailed in vitro PKS studies. The generation of hmCoA and oxCoA also suggests the potential of genetically engineering PKSs to produce sugar derivatives.

The hydrophobic residues V188 and M291 adjacent to the α -methyl group of (2R)-mmCoA, as observed in the mmCoA/AMP/MatB ternary complex, likely influence the promiscuity of MatB for α -substituted malonate derivatives and may explain why *S. coelicolor* MatB was unable to synthesize aminomalonyl-CoA (Figure 3H). Within A-domains, an aspartate is usually positioned in the A4 core motif to ionically interact with the amino group of a selected amino acid; within MatB, this position is occupied by V188. The chemical incompatibility of a valine

side chain with a charged amino group may preclude the formation of aminomalonyl-CoA. A structural alignment of MatB with a D-alanine:D-alanyl carrier protein ligase (PDB code: 3E7W) suggests that the MatB mutant V144D would bind aminomalonnate and catalyze the formation of aminomalonyl-CoA (Figures 5A and 5B). We have not tested for the formation of the less commonly utilized extender units propylmalonyl-CoA or chloroethylmalonyl-CoA; however, if MatB is not capable of selecting the corresponding diacids, appropriate mutagenesis of V188 and M291 may enable the formation of these extender units.

Thus, an enzymatic means to produce CoA-, PANT-, and SNAC-linked polyketide extender units is provided. This reaction may be utilized by many PKS laboratories to produce significant quantities of extender units, especially when they are economically unviable or commercially unavailable. The utility of MatB for in vitro PKS reactions was demonstrated not only through the incorporation of the methylmalonyl groups of mmCoA, mmPANT, and mmSNAC by a PKS module to form a polyketide product but also through the ability to observe reaction progress by monitoring the production of the coupled product, mmSNAC. The MatB ternary product complexes have provided chemical insights into the malonyl-CoA synthetase reaction as well as structural insights into substrate promiscuity. Efforts to alter the stereochemistry of α -substituted extender unit products will most likely not be successful due to the hypothesized geometry of the adenylate intermediate; however, the range of the sizes and chemistries of α -substituents of malonate derivatives ligated by MatB is quite large, and apparently only limited by the nearby residues V188 and M291.

SIGNIFICANCE

We have demonstrated the use of *Streptomyces coelicolor* MatB to enzymatically synthesize five polyketide extender units (malonyl-, methylmalonyl-, ethylmalonyl-, hydroxymalonyl-, and methoxymalonyl-CoA), of which some are commercially-unavailable or economically-prohibitive. This is the first report of enzymatic synthesis of hydroxymalonyl-CoA and methoxymalonyl-CoA. In addition to the

synthesis of these five natural extender units, we have enzymatically synthesized the corresponding D-pantetheine (PANT) and N-acetylcysteamine (SNAC) extender units. Furthermore, we demonstrated the use of (2S)-methylmalonyl-CoA, (2S)-methylmalonyl-PANT, and (2S)-methylmalonyl-SNAC to form a triketide pyrone in vitro using the final module and thioesterase of 6-deoxyerythronolide B synthase. We have also developed a coupled assay to monitor the progress of in vitro PKS reactions via HPLC, which proves faster and more economical than methods previously employed, such as radio-TLC or LC/MS. The structures of two ternary product complexes were determined: one with malonyl-CoA and AMP bound (1.45 Å) and another with (2R)-methylmalonyl-CoA and AMP bound (1.43 Å). Both ternary structures have provided insights into substrate interactions, increasing the knowledge for this subfamily of the adenylate-forming enzyme superfamily. This research marks great progress toward preparative, economical, in vitro, enzymatic synthesis of polyketides.

EXPERIMENTAL PROCEDURES

Cloning

The *matB* gene was amplified from *S. coelicolor* genomic DNA using primers 5'-TCGATTGCACATATGCTCTCTCTCCCGCCCTCT-3' and 5'-ATCGGATAGCTCGAGTCAAGTACACGGTTCAGCGCCCGCTT-3'. The gene encoding methylmalonyl-CoA epimerase was amplified from *S. coelicolor* genomic DNA using primers 5'-ATCCCGAATCATATGCTGACGCGAATCGACCA-3' and 5'-TTAGTCTGGCTCGAGTCAAGTCTCAGGTGACTCAA-3'. Fragments were digested with *NdeI* and *XhoI* (italicized) and ligated into pET28b plasmid between the corresponding restriction sites. Plasmid design allowed for the incorporation of a stop codon (underlined) at the 3' terminus of the DNA encoding both MatB and methylmalonyl-CoA epimerase. Synthetic DNA encoding the N-terminal docking domain from DEBS3 fused to the sixth module and thioesterase from DEBS3 was a gift from Kosan Biosciences (Menzella et al., 2005). The DNA was digested at the flanking *NdeI* and *EcoRI* restriction sites and ligated into pET28b.

Protein Expression and Purification

MatB and methylmalonyl-CoA epimerase expression plasmids were transformed into *Escherichia coli* BL21(DE3), whereas the Mod6TE expression vector was transformed into *E. coli* K207-3 cells (Murlı et al., 2003). Starter cultures (50 ml) were grown overnight and used to inoculate prewarmed (37°C) Luria broth, supplemented with 50 mg/L kanamycin. When OD₆₀₀ = 0.4, the media was cooled (15°C) and protein expression was induced with 0.5 mM IPTG. After 16 hr, cells were harvested by centrifugation, resuspended in lysis buffer (10% glycerol, 0.5 M NaCl, 100 mM HEPES pH 7.5), sonicated, and centrifuged (30,000 relative centrifugal force for 45 min) to remove cellular debris. Cell-free lysate was passed over a nickel-NTA column equilibrated with lysis buffer. The column was washed with lysis buffer containing 15 mM imidazole and protein was eluted using lysis buffer containing 150 mM imidazole. Final protein concentrations were determined using a Thermo Scientific Nano-drop 1000.

MatB was further purified for crystallization via gel filtration using a Superdex 200 column equilibrated in gel filtration buffer (10% glycerol, 150 mM NaCl, and 10 mM HEPES pH 7.5). By comparison to a gel filtration standard (Bio-Rad), MatB eluted as a ~50 kDa monomer. Fractions were collected and concentrated to 15 mg/ml in gel filtration buffer (Millipore Centrifugal Filter Unit, 30 kDa MWCO). The final protein concentration was determined by using a Thermo Scientific Nanodrop 1000.

The same purification protocol was followed for selenomethionine-labeled MatB (Se-MatB); however, growth and expression conditions differed. Each liter of M9 growth medium contained 6 g Na₂HPO₄, 3 g KH₂PO₄, 500 mg NaCl, 1 g NH₄Cl, 0.1 mM CaCl₂, 1 mM MgSO₄, 0.4% glucose, and 20 mg kanamycin. Prewarmed (37°C) media was inoculated with saturated starter culture

(3 ml). When the OD₆₀₀ = 0.4, each liter of media was supplemented with lysine, phenylalanine, and threonine (each 100 mg), isoleucine, leucine, and valine (each 50 mg), and selenomethionine (60 mg). After 15 min protein expression was induced with 0.5 mM IPTG. The cultures were then cooled (15°C) and after 16 hr cells were harvested. Protein purification, gel filtration, and concentration of Se-MatB protein followed the methods described above.

Protein Crystallization

The following conditions were used for the protein solution of mmCoA/AMP-bound selenomethionine-labeled MatB: 15.8 mg/ml Se-MatB, 1 mM CoA, 5 mM methylmalonate pH 7.5, 1 mM ATP, 2 mM DTT, and 5 mM MgCl₂. Optimal mmCoA/AMP-bound selenomethionine-labeled MatB crystals grew overnight in 31% PEG 4000, 100 mM MgCl₂, and 100 mM Tris-HCl pH 7.5 via sitting drop vapor diffusion at 22°C with a protein solution to crystallization buffer ratio of 1:1. The following conditions were used for the protein solution of mCoA/AMP-bound MatB: 10 mg/ml MatB, 20 mM CoA, 24 mM sodium malonate pH 7.7, 24 mM ATP, and 48 mM MgCl₂. Optimal mCoA/AMP-bound MatB crystals grew overnight in 35% PEG 4000, 100 mM MgCl₂, and 100 mM Tris-HCl pH 8.2 via sitting drop vapor diffusion at 22°C with a protein solution to crystallization buffer ratio of 1:1. The following conditions were used for the protein solution of mmCoA/AMP-bound MatB: 9.6 mg/ml MatB, 20 mM CoA, 24 mM sodium methylmalonate pH 7.5, 24 mM ATP, and 48 mM MgCl₂. Optimal mmCoA/AMP-bound MatB crystals were grown overnight in 33% PEG 4000, 100 mM MgCl₂, and 100 mM Tris-HCl pH 9.5 via sitting drop vapor diffusion at 22°C with a protein solution to crystallization buffer ratio of 1:1.

Data Collection, Processing, and Refinement

Diffraction data were collected at ALS beamline 5.0.2, then integrated and scaled using HKL2000 (Otwinowski and Minor, 1997). The structure of mmCoA/AMP-bound selenomethionine-labeled MatB was solved by single-wavelength anomalous dispersion using Phenix (Adams et al., 2002). This structure was used as a search model for molecular replacement using Phaser (CCP4, 1994), yielding the solutions for both mCoA/AMP-bound MatB and mmCoA/AMP-bound MatB. Water molecules were identified using Coot (F_o-F_c map contoured at $\sigma = 3.0$) (Emsley and Cowtan, 2004). Refinement cycles using Coot (Emsley and Cowtan, 2004) and Refmac5 (CCP4, 1994) were performed until the R-factors could no longer be improved (Table 1). Figures were prepared using PyMol (DeLano, 2002) and LIGPLOT (Wallace et al., 1995).

Synthesis of N-Acetylcysteamine

A total of 1.14 g cysteamine hydrochloride (10.0 mmol, 1.0 eq.), 0.56 g KOH (10.0 mmol, 1.0 eq.), and 2.52 g NaHCO₃ (30.0 mmol, 3.0 eq) was dissolved in a round-bottom flask containing 50 ml water. After the dropwise addition of 0.95 ml acetic anhydride (10.0 mmol, 1.0 eq.), the solution was stirred at 22°C for 10 min. The pH was then adjusted to 7.3 using 12.1 N HCl. The resulting mixture was extracted with 150 ml ethyl acetate. The organic layer was dried using MgSO₄, and after filtration a quantitative yield of N-acetylcysteamine was isolated in vacuo. ¹H-NMR (CDCl₃) 400 MHz, δ (ppm): 5.97 (1H, bs), 3.40 (2H, q, J = 8.0), 2.65 (2H, m, J = 8.4), 1.98 (3H, s), 1.33 (1H, t, J = 8.8).

Synthesis of Methoxymalonic Acid

A total of 0.850 ml dimethyl methoxymalonate (6.2 mmol, 1.0 eq.) and 2.4 g NaOH (60 mmol, 9.7 eq.) was dissolved in a round-bottom flask containing 10 ml water. The resulting solution was stirred at 65°C overnight. The solution was then acidified with 10 ml 12.1 N HCl and extracted with 30 ml ethyl acetate. The organic layer was dried using MgSO₄, and after filtration a quantitative yield of methoxymalonic acid was isolated in vacuo.

Formation of D-Pantetheine

D-pantetheine (0.021 mmol, 1.0 eq.) and DTT (0.022 mmol, 1.0 eq.) were dissolved in 100 μ l 20% (w/v) glycerol (aq.). The solution was incubated at 60°C for 15 min., and the resulting D-pantetheine solution was stored at 22°C.

HPLC Analysis of MatB Reactions

Enzymatic reactions to generate extender units were set up using the following conditions: 6 nM MatB, 0.55 mM CoA or 1.0 mM D-pantetheine or 4.2 mM

SNAC, 1.3 mM ATP, 22 mM malonate derivative, 9 mM MgCl₂, 15% (w/v) glycerol, and 100 mM HEPES pH 7.5. All reactions were incubated at 22°C overnight. Samples were analyzed by HPLC (Waters) using a Varian Microsorb-MV 300-5 C₁₈ column and a Waters 2998 photodiode array detector. The mobile phases consisted of water containing 0.1% TFA (solvent A) and methanol containing 0.1% TFA (solvent B). A linear gradient (flow rate = 1 ml/min) of 0%–67% B over 20 min was used for sample analysis. Reactions were monitored at 254 nm (adenine, CoA) or 235 nm (thioester bond, SNAC, and PANT compounds).

HPLC Analysis of Triketide Pyrone Reactions

MatB reactions were set up using the following conditions: 5 mM CoA or 5 mM D-pantetheine or 5 mM SNAC, 100 mM HEPES pH 7.5, 100 mM MgCl₂, 20 mM ATP (in 100 mM HEPES pH 7.5), 50 mM sodium methylmalonate pH 7.2, 10% glycerol, and 8 nM MatB. Reactions were incubated at 22°C overnight and analyzed by HPLC to ensure formation of mmCoA, mmPANT, or mmSNAC (see HPLC Analysis of MatB Reactions). Mod6TE reactions were set up by adding (2S, 3R)-2-methyl-3-oxopentanoate-SNAC (diketideSNAC) (10 mM, final), *S. coelicolor* methylmalonyl-CoA epimerase (12 nM, final), and Mod6TE (4 nM, final) to the MatB reaction, so that the MatB reaction was diluted 2-fold. Reactions were incubated at 22°C for 1 day. Samples were analyzed by HPLC (Waters) using a Varian Microsorb-MV 300-5 C₁₈ column and a Waters 2998 photodiode array detector. The mobile phases consisted of water containing 0.1% TFA (solvent A) and methanol containing 0.1% TFA (solvent B). A linear gradient (flow rate = 1 ml/min) of 0%–100% B over 15 min was used. Reactions were monitored at 254 nm (adenine, CoA), 235 nm (thioester bond, SNAC, and PANT compounds), and 290 nm (triketide pyrone).

Mass Spectrometry Analysis

CoA-linked extender units were collected from HPLC runs and isolated in vacuo. Samples were subjected to low-resolution negative-ESI mass spectrometry performed with a Finnigan LCQ ion trap mass spectrometer with the needle voltage set to 3 kV and the capillary temperature set to 120°C (Figure 2A).

LC/MS Analysis

The triketide pyrone and two products from the hmSNAC reaction were collected, isolated in vacuo, resuspended in 25% acetonitrile and 0.1% formic acid, and subjected to positive-ESI LC/MS (Agilent Technologies 1200 Series HPLC with a Gemini C₁₈ column coupled to an Agilent Technologies 6130 quadrupole mass spectrometer). Mobile phases consisted of water containing 0.1% formic acid (solvent A) and acetonitrile containing 0.1% formic acid (solvent B). A linear gradient (flow rate = 0.7 ml/min) of 5%–95% B over 12 min was used (Figure 2C).

ACCESSION NUMBERS

Coordinates were deposited with PDB Codes 3NYR and 3NYQ for mCoA/AMP-bound and mmCoA/AMP-bound MatB, respectively.

ACKNOWLEDGMENTS

We would like to acknowledge Darren Gay for helping optimize the MatB ternary product complex crystals and Art Monzingo for organizing data collection at ALS Beamline 5.0.2. We would also like to thank the Macromolecular Crystallography and Mass Spectrometry Facilities at the University of Texas at Austin. Funding was provided by the Robert A. Welch Foundation.

Received: October 1, 2010

Revised: November 25, 2010

Accepted: December 2, 2010

Published: February 24, 2011

REFERENCES

Adams, P.D., Grosse-Kunstleve, R.W., Hung, L.W., Ioerger, T.R., McCoy, A.J., Moriarty, N.W., Read, R.J., Sacchettini, J.C., Sauter, N.K., and Terwilliger, T.C.

(2002). PHENIX: building new software for automated crystallographic structure determination. *Acta Crystallogr. D Biol. Crystallogr.* 58, 1948–1954.

Carroll, B.J., Moss, S.J., Bai, L.Q., Kato, Y., Toelzer, S., Yu, T.W., and Floss, H.G. (2002). Identification of a set of genes involved in the formation of the substrate for the incorporation of the unusual “glycolate” chain extension unit in ansamitocin biosynthesis. *J. Am. Chem. Soc.* 124, 4176–4177.

CCP4 (Collaborative Computational Project, Number 4). (1994). The CCP4 suite: programs for protein crystallography. *Acta Crystallogr. D Biol. Crystallogr.* 50, 760–763.

Chan, Y.A., and Thomas, M.G. (2010). Recognition of (2S)-aminomalonyl-acyl carrier protein (ACP) and (2R)-hydroxymalonyl-ACP by acyltransferases in Zwittermicin A biosynthesis. *Biochemistry* 49, 3667–3677.

Chan, Y.A., Podevels, A.M., Kevany, B.M., and Thomas, M.G. (2009). Biosynthesis of polyketide synthase extender units. *Nat. Prod. Rep.* 26, 90–114.

Conti, E., Stachelhaus, T., Marahiel, M.A., and Brick, P. (1997). Structural basis for the activation of phenylalanine in the non-ribosomal biosynthesis of gramicidin S. *EMBO J.* 16, 4174–4183.

Dayem, L.C., Carney, J.R., Santi, D.V., Pfeifer, B.A., Khosla, C., and Kealey, J.T. (2002). Metabolic engineering of a methylmalonyl-CoA mutase–epimerase pathway for complex polyketide biosynthesis in *Escherichia coli*. *Biochemistry* 41, 5193–5201.

DeLano, W.L. (2002). The PyMOL Molecular Graphics System User's Manual (San Carlos, CA: DeLano Scientific).

Emsley, P., and Cowtan, K. (2004). COOT: model-building tools for molecular graphics. *Acta Crystallogr. D Biol. Crystallogr.* 60, 2126–2132.

Jogl, G., and Tong, L. (2004). Crystal structure of yeast acetyl-coenzyme A synthetase in complex with AMP. *Biochemistry* 43, 1425–1431.

Gao, X., Wang, P., and Tang, Y. (2010). Engineered polyketide biosynthesis and biocatalysis in *Escherichia coli*. *Appl. Microbiol. Biotechnol.* 10.1007/s00253-010-2860-4.

Gokhale, R.S., Tsuji, S.Y., Cane, D.E., and Khosla, C. (1999). Dissecting and exploiting intermodular communication in polyketide synthases. *Science* 284, 482–485.

Gulick, A.M., Starai, V.J., Horswill, A.R., Homick, K.M., and Escalante-Semerena, J.C. (2003). The 1.75 Å crystal structure of acetyl-CoA synthetase bound to adenosine-5'-propylphosphate and coenzyme A. *Biochemistry* 42, 2866–2873.

Gulick, A.M., Lu, X., and Dunaway-Mariano, D. (2004). Crystal structure of 4-chlorobenzoate:CoA Ligase/synthetase in the unliganded and aryl substrate-bound states. *Biochemistry* 43, 8670–8679.

Herzberg, O., and Moul, J. (1991). Analysis of the steric strain in the polypeptide backbone of protein molecules. *Proteins* 11, 223–229.

Hisanaga, Y., Ago, H., Nakagawa, N., Hamada, K., Ida, K., Yamamoto, M., Hori, T., Arii, Y., Sugahara, M., Kuramitsu, S., et al. (2004). Structural basis of the substrate-specific two-step catalysis of long chain fatty acyl-CoA synthetase dimer. *J. Biol. Chem.* 279, 31717–31726.

Keatinge-Clay, A.T. (2007). A tylosin ketoreductase reveals how chirality is determined in polyketides. *Chem. Biol.* 14, 898–908.

Khosla, C., Tang, Y., Chen, A.Y., Schnarr, N.A., and Cane, D.E. (2007). Structure and mechanism of the 6-deoxyerythronolide B synthase. *Annu. Rev. Biochem.* 76, 195–221.

Kochan, G., Pilka, E.S., von Delft, F., Oppermann, U., and Yue, W.W. (2009). Structural snapshots for the conformation-dependent catalysis by human medium-chain acyl-coenzyme A synthetase ACSM2A. *J. Mol. Biol.* 388, 997–1008.

Lee, T.V., Johnson, L.J., Johnson, R.D., Koulman, A., Lane, G.A., Lott, J.S., and Arcus, V.L. (2010). Structure of a eukaryotic nonribosomal peptide synthetase adenylation domain that activates a large hydroxamate amino acid in siderophore biosynthesis. *J. Biol. Chem.* 285, 2415–2427.

Marahiel, M.A. (2009). Working outside the protein-synthesis rules: insights into non-ribosomal peptide synthesis. *J. Pept. Sci.* 15, 799–807.

- Marahiel, M.A., Stachelhaus, T., and Mootz, H.D. (1997). Modular peptide synthetases involved in nonribosomal peptide synthesis. *Chem. Rev.* **97**, 2651–2674.
- Menzella, H.G., Reid, R., Carney, J.R., Chandran, S.S., Reisinger, S.J., Patel, K.G., Hopwood, D.A., and Santi, D.V. (2005). Combinatorial polyketide biosynthesis by de novo design and rearrangement of modular polyketide synthase genes. *Nat. Biotechnol.* **23**, 1171–1176.
- Mootz, H.D., Schwarzer, D., and Marahiel, M.A. (2002). Ways of assembling complex natural products on modular nonribosomal peptide synthetases. *ChemBioChem* **3**, 490–504.
- Murli, S., Kennedy, J., Dayem, L.C., Carney, J.R., and Kealey, J.T. (2003). Metabolic engineering of *Escherichia coli* for improved 6-deoxyerythronolide B production. *J. Ind. Microbiol. Biotechnol.* **30**, 500–509.
- Nakatsu, T., Ichiyama, S., Hiratake, J., Saldanha, A., Kobashi, N., Sakata, K., and Kato, H. (2006). Structural basis for the spectral difference in luciferase bioluminescence. *Nature* **440**, 372–376.
- Otwinowski, Z., and Minor, W. (1997). Processing of X-ray diffraction data collected in oscillation mode. *Methods Enzymol.* **276**, 307–326.
- Pfeifer, B.A., and Khosla, C. (2001). Biosynthesis of polyketides in heterologous hosts. *Microbiol. Mol. Biol. Rev.* **65**, 106–118.
- Pohl, N.L., Gokhale, R.S., Cane, D.E., and Khosla, C. (1998). Synthesis and incorporation of an N-acetylcysteine analogue of methylmalonyl-CoA by a modular polyketide synthase. *J. Am. Chem. Soc.* **120**, 11206–11207.
- Pohl, N.L., Hans, M., Lee, H.Y., Kim, Y.S., Cane, D.E., and Khosla, C. (2001). Remarkably broad substrate tolerance of malonyl-CoA synthetase, an enzyme capable of intracellular synthesis of polyketide precursors. *J. Am. Chem. Soc.* **123**, 5822–5823.
- Reger, A.S., Carney, J.M., and Gulick, A.M. (2007). Biochemical and crystallographic analysis of substrate binding and conformational changes in acetyl-CoA synthetase. *Biochemistry* **46**, 6536–6546.
- Reger, A.S., Wu, R., Dunaway-Mariano, D., and Gulick, A.M. (2008). Structural characterization of a 140 degrees domain movement in the two-step reaction catalyzed by 4-chlorobenzoate:CoA ligase. *Biochemistry* **47**, 8016–8025.
- Shah, M.B., Ingram-Smith, C., Cooper, L.L., Qu, J., Meng, Y., Smith, K.S., and Gulick, A.M. (2009). The 2.1 Å crystal structure of an acyl-CoA synthetase from *Methanosarcina acetivorans* reveals an alternate acyl-binding pocket for small branched acyl substrates. *Proteins* **77**, 685–698.
- Stachelhaus, T., Mootz, H.D., and Marahiel, M.A. (1999). The specificity-conferring code of adenylation domains in nonribosomal peptide synthetases. *Chem. Biol.* **6**, 493–505.
- Staunton, J., and Wilkinson, B. (2001). Combinatorial biosynthesis of polyketides and nonribosomal peptides. *Curr. Opin. Chem. Biol.* **5**, 159–164.
- Strieker, M., Tanovic, A., and Marahiel, M.A. (2010). Nonribosomal peptide synthetases: structures and dynamics. *Curr. Opin. Struct. Biol.* **20**, 234–240.
- Tang, Y., Kim, C.-Y., Mathews, I.I., Cane, D.E., and Khosla, C. (2006). The 2.7-Å crystal structure of a 194-kDa homodimeric fragment of the 6-deoxyerythronolide B synthase. *Proc. Natl. Acad. Sci. USA* **103**, 11124–11129.
- Wallace, A.C., Laskowski, R.A., and Thornton, J.M. (1995). LIGPLOT: a program to generate schematic diagrams of protein-ligand interactions. *Protein Eng.* **8**, 127–134.
- Walsh, C.T. (2004). Polyketide and nonribosomal peptide antibiotics: modularity and versatility. *Science* **303**, 1805–1810.
- Wang, M., Opare, P., and Boddy, C.N. (2009). Polyketide synthase thioesterases catalyze rapid hydrolysis of peptidyl thioesters. *Bioorg. Med. Chem. Lett.* **19**, 1413–1415.
- Wu, R., Cao, J., Lu, X., Reger, A.S., Gulick, A.M., and Dunaway-Mariano, D. (2008). Mechanism of 4-chlorobenzoate:coenzyme A ligase catalysis. *Biochemistry* **47**, 8026–8039.
- Yonus, H., Neumann, P., Zimmermann, S., May, J.J., Marahiel, M.A., and Stubbs, M.T. (2008). Crystal structure of DltA. *J. Biol. Chem.* **283**, 32484–32491.